

MELTING AND SOLIDIFICATION STUDIES BY ADVANCED THERMAL ANALYSIS OF CAST IRON

***L. Battezzati, *M. Baricco, *F. Marongiu - **G. Serramoglia, **D. Bergesio**
***Dipartimento di Chimica I.F.M. e Unità INFM, Università di Torino**
****Teksid, Crescentino (Vercelli)**

Abstract

A tool widely employed in foundry is measuring the melt temperature during free cooling in cups. Thermal analysis curves provide information on liquidus, eutectic, solidus temperatures and recalescence effects. More advanced analyses can be performed in the laboratory using differential devices where a temperature program is imposed to both the sample and an inert reference. The sensitivity in the detection of temperature points is enhanced and quantitative determination of the heat release during solidification, and therefore of the solid fraction, becomes feasible.

In this work we have employed a high temperature differential scanning calorimeter (Setaram HTDSC) capable of reaching temperatures up to 1600 °C to follow melting and solidification of master alloys for the production of lamellar, compact graphite and spheroidal cast irons, at various heating and cooling rates under protective helium atmosphere. Binary Fe-C alloys prepared in the laboratory with composition of 4.3 wt% C were analysed as well. The solid fraction as a function of temperature is obtained by integration of the DSC traces. The correlation between thermal data obtained by HTDSC, free cooling in cups and microstructure is shown.

INTRODUCTION

The microstructural control in castings is of paramount relevance in processing of advanced alloys. In fact, the microstructure of any material will depend on the thermal history via a complex interplay of different, though related, events, e.g. heat transfer, imposed temperature gradient, undercooling, nucleation and growth rates, segregation effects [1]. The classical technique devised to follow the ensemble of processes is thermal analysis since the early development of solidification as a science [2]. Actually, measuring the material temperature during free cooling in cups is a tool widely employed in foundry practice to date. Thermal analysis curves provide information on liquidus, eutectic, solidus temperatures, recalescence effects [3]. More advanced analyses can be performed in the laboratory using differential devices where a temperature program is

Riassunto

Una tecnica analitica ampiamente utilizzata in fonderia consiste nel misurare la temperatura del fuso durante il suo raffreddamento libero in coppette contenenti una termocoppia. Le curve di analisi termica così ottenute forniscono informazioni circa le temperature di liquidus, di solidificazione eutettica, di solidus, e sulla recalescenza. Analisi più sofisticate possono essere effettuate in laboratorio utilizzando strumenti di tipo "differenziale" nei quali risultano possibili stime quantitative dei calori latenti di solidificazione, nonché delle frazioni di solido.

In questo lavoro abbiamo impiegato un calorimetro differenziale a scansione ad alta temperatura (Setaram HTDSC) in grado di raggiungere temperature oltre i 1600°C e di seguire la fusione e la solidificazione di leghe per la produzione di ghise a grafite lamellare, compatta e sferoidale a diverse velocità di riscaldamento e di raffreddamento in atmosfera d'elio. Sono state preparate ed analizzate anche leghe binarie Fe-C al 4.3% in peso. Si è ottenuta la frazione di solido in funzione della temperatura mediante integrazione dei tracciati DSC. Si mostra la correlazione fra i dati di analisi termica ottenuti mediante HTDSC, il raffreddamento libero in coppette e la microstruttura.

imposed to both the sample and an inert reference. The sensitivity in the detection of temperature points is enhanced and quantitative determination of the heat release during solidification, and therefore of the solid fraction, becomes feasible [4, 5].

We have developed a methodology for the study of Fe-B, Ni-B and Fe-Si-B melts (i. e. glass-forming alloys) employing a high temperature differential scanning calorimeter. Temperatures and heat of solidification of both stable and metastable phases and eutectics were determined allowing full description of the phase diagrams including the metastable undercooling regime [6]. The technique is extended here to the microstructural control of cast irons.

The aim of the work is twofold: to compare the results obtained with conventional and advanced thermal analysis and to provide a quantitative basis for prediction of the microstructures in castings.

EXPERIMENTAL

In this work we have employed a high temperature differential scanning calorimeter (Setaram HTDSC) capable of reaching temperatures up to

1600 °C to follow melting and solidification of several irons at various heating and cooling rates. It consists of twin alumina cells surrounded by Pt-13% Rh thermopiles which are inserted in a graphite furnace. The samples (100-400 mg) have been introduced in the crucible together with alumina powder in order to avoid sticking to the crucible walls. After repeated evacuation and filling with He, a constant flow of pure He has been sent in the calorimetric cell in order to guarantee a protected atmosphere during the experiments. Helium is used to enhance the sensitivity of the device due to its high thermal conductivity. Heating and cooling rates were 10 K/min.

Binary Fe-C alloys in the form of buttons of about 50 g in weight were then prepared in the laboratory with composition of 4.3 wt% C by arc melting the appropriate mixture of pure elements. It was analysed in HTDSC to provide a basis for a correlation between thermal analysis curves and phase transformations.

RESULTS AND DISCUSSION

The analysis will be illustrated via examples pertaining to two cast irons, named A2 and C2, which were inoculated with the same amount of Fe-Si (0.1 wt%). One was also added with 0.32 wt% spheroidizing agent. Their microstructure is shown in Fig. 1a and Fig. 1b respectively. They display clear differences in the morphology of graphite as expected in conventional or modified cast irons. In Fig. 1a a few dendrite branches also appear.

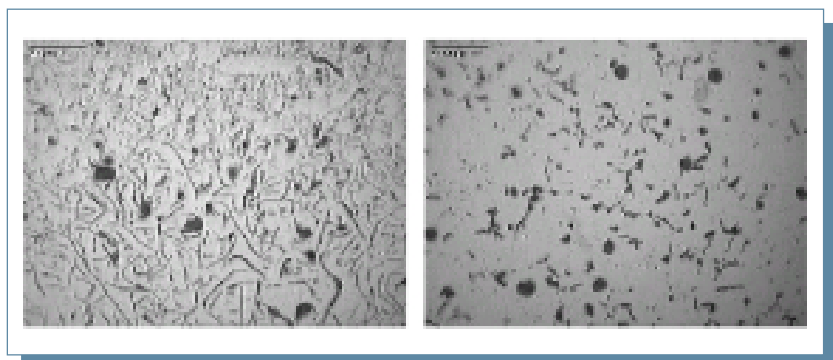


Fig. 1a: Microstructure of A2 cast iron - Fig. 1b: Microstructure of C2 cast iron

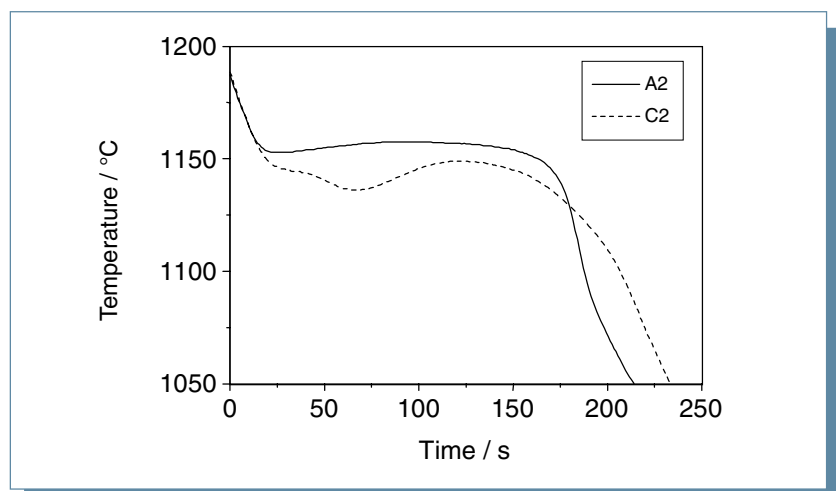


Fig. 2: Thermal analysis curves for A2 and C2 irons

Industrial castings were analysed both in the laboratory and in the foundry. The samples came from a batch of master alloy (3.70 wt% C, 1.87 wt% Si, 0.010 wt% S) which was subdivided in twelve ladles each weighting about one ton. Groups of ladle charges were added with selected amounts of an Fe-Si inoculant (0.05, 0.1 and 0.2 wt%) and of an Fe-Ni-Mg-Ce spheroidizing agent (0.0, 0.16, 0.32, 0.48 wt%). Portions of the molten alloys were withdrawn and poured into commercial cups containing a thermocouple. The thermocouple output has been analysed with a commercial software (ATAS) [7].

Optical microscopy was employed to observe the microstructures.

Wide white areas in Fig. 1b indicate the occurrence of primary dendrites. Some nodules are spherical but several graphite aggregates are vermicular. The microstructure is typical of compact graphite irons due to the amount of inoculants added to the alloy in the ladle.

Fig. 2 shows the thermal analysis curves obtained during solidification of A2 and C2 irons in the foundry.

The cup where the melt is poured contains roughly 350 g. The thermocouple in its centre senses the average change in temperature of the surrounding. Selected data are collected in Tab. 1. They are diverse for the two irons confirming that thermal analysis is a suitable technique for prediction of microstructures.

Curve A2 has no discernible liquidus arrest. The change in slope of the curve marks the eutectic start, $T_{E,s}$, in that eutectic solidification begins in the sample, possibly on the cup walls, latent heat is released in the melt compensating for the heat lost because of free cooling. While most of the melt is still liquid and undercools, the average temperature reaches a minimum, called the minimum eutectic temperature, $T_{E,min}$. Massive solidification now occurs rising the temperature of the sample to the "maximum eutectic temperature", $T_{E,max}$, where it stays until freezing approaches completion. The latter temperature should be close to the equilibrium eutectic of the phase diagram. In the last stage of cooling, the temperature drops fast. The curve has an inflection point which is taken as the end of solidification, T_{sol} , in that it marks the end of the detection by the thermocouple of the release of latent heat.

Fig. 3 shows the HTDSC traces obtained with samples of alloys A2 and C2. The tiny cusps occurring at 740 °C are due to the ferro-paramag-

netic transition of the ferrite. Its temperature is fully compatible with the amount of Si dissolved in α -Fe [8]. For A2 the subsequent endothermic peak signals the metastable eutectoid transformation. The iron is actually mostly pearlitic. The peak has a shoulder on the high temperature side since part of the material undergoes a stable eutectoid transformation. The melting onset, T_f , occurs at 1157 °C. However the curve starts deflecting progressively from the baseline at a lower temperature. With the heating rate employed in this work the melting peak extends over some forty degrees so no liquidus point can be detected.

The cooling trace shows clearly a primary solidification signal at $T_{L,und}$ followed by the main eutectic endothermic event, $T_{E,und}$. For a DSC trace of solidification starting at a liquidus point a progressive deflection from the baseline is expected before attaining a peak, instead of the sharp peak found here. It was earlier shown that a peak occurs when crystallisation takes place abruptly in an undercooled melt. Therefore the liquidus derived from the DSC trace is a lower estimate of the actual liquidus point. The sharpness of the peak and its height are a measure of the extent of undercooling [6]. In the present case the peak is shallow so the undercooling should be limited to a few degrees. The eutectic solidification starts well below the melting onset recorder earlier, i. e. the eutectic is undercooled although coexisting with austenite dendrites. This is not surprising since austenite is not a good catalyst for graphite nucleation [9]. In other experiments when we dealt with hypereutectic irons, the eutectic did solidify at the equilibrium temperature. The eutectic onset on cooling is definitely lower than the “minimum eutectic temperature” obtained with the cup. The evidences collected with HTDSC experiments refer to solidification of small samples in a calorimetric cell and will represent the behaviour of portions of a bulk volume of melt and not the average behaviour of the material as that contained in the cup described above. On the other hand, more details are detected such as dendrite formation. Note also that the end of solidification is very close in the two experiments. The latent heat of melting and solidification is derived by integration of the signal via a calibration curve of the instrument obtained by melting pure elements. It amounts to 225 J/g in the present case. Finally, the eutectoid transformation on cooling appears highly undercooled. The signal is much larger in area than that corresponding to the same transformation on heating. It may be shown that this is compatible with transformation of austenite

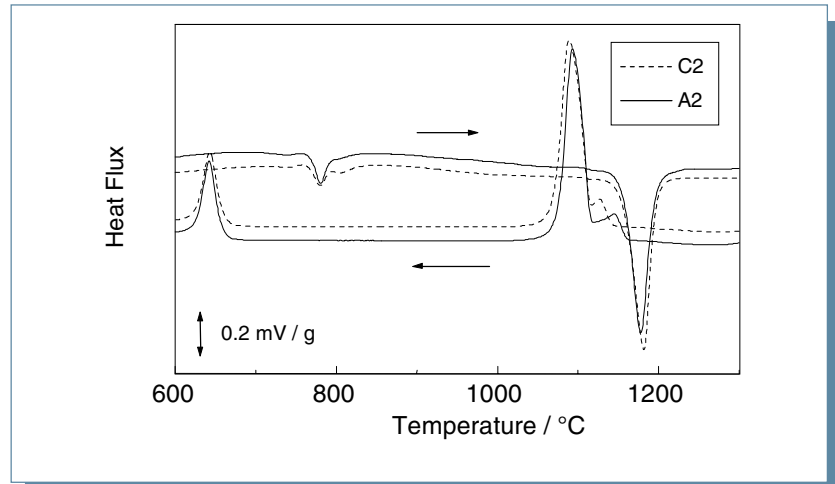


Fig. 3: HTDSC traces for A2 and C2 cast irons

at temperatures lower than equilibrium.

Considering now curve C2 in Fig. 2, the liquidus arrest, T_L , is well defined and the bulk undercooling well pronounced reaching 1136 °C. Recalescence and the consequent dissipation of heat are larger than for A2 so a sharp eutectic arrest is not produced. The end of solidification is not clearly defined. The shape of the curve is common to all irons having compact graphite.

The HTDSC trace for C2 in Fig. 3 has two peaks for the eutectoid showing both metastable and stable transformations. The melting onset is at 1154 °C, a datum which could not be obtained from the thermal analysis curve of Fig. 2. On cooling the trace must have lost information due to fading of the spheroidizing agent. There is, however, clear evidence of dendritic solidification of austenite and of eutectic undercooling. The end of solidification is well recognised. It occurs in the temperature range also evidenced in Fig. 2. The overall heat of solidification is 220 J/g.

In order to show the effect of an increase in the amount of inoculant added to the iron, we report in Fig. 4 a comparison between the HTDSC traces of irons A2 and A3 (added with 0.2% Fe-Si). The microstructure of A3, mostly ferritic, is characterised by finer flakes of graphite with respect to A2 with no evidence of austenitic dendrites. The conventional thermal analysis curve for A3 reproduces that of A2 within the experimental uncertainty (not reported). Also the melting onset obtained in HTDSC is reproduced at $T_f = 1158$ °C as well as the eutectic undercooling and the end of solidification. The two traces differ only for the shift of 22 °C of the primary solidification peak for A3 which is barely visible. It is concluded that with the HTDSC technique finer details of the solidification path can be revealed with respect to conventional thermal analysis.

TABLE 1. SELECTED TEMPERATURE DATA (ALL IN °C) FOR MELTING AND SOLIDIFICATION OF THE IRONS DESCRIBED IN THE TEXT. THEY WERE OBTAINED BY CONVENTIONAL THERMAL ANALYSIS AND HTDSC (ITALICS).

Iron	T_L	$T_{L,und}$	$T_{E,s}$	$T_{E,min}$	$T_{E,MAX}$	T_f	$T_{E,und}$	T_{sol}	T_{sol}
A2	-	1165	1153	1153	1158	1162	1135	1114	1102
A3	-	1143	1151	1153	1158	1158	1135	1116	1105
C2	1145	1142	1140	1136	1149	1154	1115	(1083)	1070

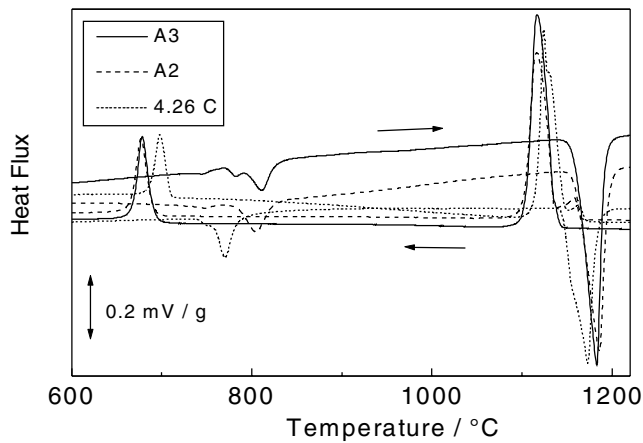


Fig. 4: HTDSC traces for three cast irons

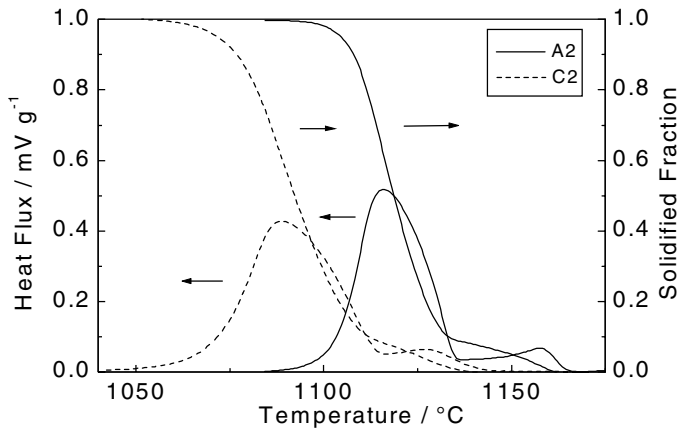


Fig. 5: HTDSC traces and solidified fraction for A2 and C2 irons

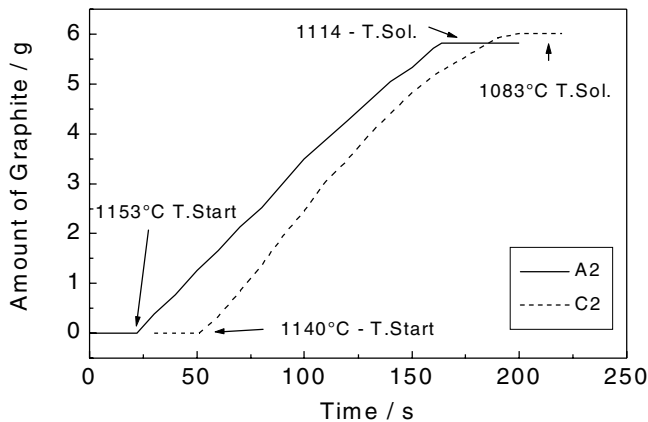


Fig. 6: Amount of graphite as a function of solidification time in A2 and C2 cast irons as obtained from thermal analysis curves

In Fig. 4 a trace is reported also for a binary Fe-C alloy prepared in the laboratory using pure elements with composition close to the binary eutectic, to unveil further aspects of melting and solidification processes. The melting peak is doubled due to the occurrence of both metastable and stable eutectics. The onset temperature of the metastable eutectic is 1145 °C in agreement with most recent determination [10]; that of stable eutectic cannot be determined with precision in the present experiments. The beginning of solidification is sharper than for multicomponent alloys. The difference is actually expected from consideration of the respective phase diagrams. For the binary alloy, the eutectic is an invariant reaction whereas, considering C2 as a Fe-C-Si alloy, a monovariant triangle is entered on melting which must occur in a temperature range. At each temperature there is compositional partition imposed by an isothermal tie triangle. This causes a detectable effect on the shape of the trace. The binary eutectic could be fully transformed to graphite eutectic by thermal cycling around the melting point and the latent heat determined as $230 \pm 10 \text{ J/g}$ ($11.0 \pm 0.5 \text{ kJ/mol}$).

The solid fraction as a function of temperature is obtained by integration of the DSC traces and is shown in Fig 5 for A2 and C2 irons. A constant latent heat was assumed for both primary and eutectic reactions. This is justified by the estimate of the heat release for austenite solidification we performed using standard thermodynamic data [11]. It turns out of the order of 11 J/mol, to all practical purposes identical to the latent heat of the eutectic. Both integral curves are made of two zones related to solidification of primary austenite and eutectic respectively. The amount of austenite is below 10% in both alloys. The amount of eutectic is therefore above 90%. The effect of undercooling is well apparent in both the start and progress of solidification. The curve for A2 is steeper than that for C2 indicating a faster and steady development of the eutectic.

The software for thermal analysis we used in this work [7] provides a quantity related to the transformed fraction, i. e. the amount of graphite, expressed in grams, progressively formed during solidification. Curves in Fig. 6 show it as function of time. The time for full development of graphite is slightly longer for C2 and, conversely, the curve is steadier for A2. The temperatures corresponding to the start and the end of the process are marked on the figure to show the solidification interval for each alloy. The findings are in line with those of HTDSC.

CONCLUSIONS

The main results of the present work are summarised as follows:

- Differential thermal analysis data were collected for a set of cast irons. They provide full description of melting, solidification and eutectoid transformation.
- The HTDSC curves contain detailed features such as peaks related to primary austenite

solidification which may go undetected in conventional thermal analysis.

- Quantitative data for the heat of solidification and transformed fraction as a function of temperature are obtained.

ACKNOWLEDGMENTS

F. M. wishes to acknowledge INFM for providing a grant during which this work was performed.

REFERENCES

1. W. Kurz and D. J. Fischer, *Fundamentals of Solidification*, Trans Tech Publications, Aedermannsdorf, Switzerland, 1986.
2. S.W. Smith Editor, *Roberts-Austen: A record of his work*, Griffin and Co., London, 1914.
3. U. Ekpoom and R.W. Heine, *AFS Transactions*, 15 (1981) 27.
4. H. Fredriksson and B. Rogberg, *Metal Science*, 13 (1979) 685.
5. M. Baricco, L. Battezzati and P. Rizzi, *J. Alloys and Compounds*, 220 (1995) 212.
6. L. Battezzati, C. Antonione, M. Baricco, *J. Alloys and Compounds*, 247 (1997) 164.
7. ATAS® is a product of NovaCast AB, Sweden.
8. O. Kubaschewski, *Iron-Binary Phase Diagrams*, Springer Verlag, Berlin, 1982.
9. M. J. Hunter and G.A. Chadwick, *J. Iron and Steel Institute*, 210 (1972) 707.
10. P. Magnin and W. Kurz, *Z. Metallkde*, 79 (1988) 282.
11. R. Hultgren, P. D. Desai, D. T. Hawkins, M. Gleiser and K. K. Kelly, *Selected Values of the Thermodynamic Properties of Binary Alloys*, American Society for Metals, Metals Park, Ohio, 1973.